Positively Charged Deoxynucleic Methylthioureas: Synthesis and Binding Properties of Pentameric Thymidyl Methylthiourea

Dev P. Arya and Thomas C. Bruice*

Contribution from the Department of Chemistry, University of California, Santa Barbara, California 93106

Received August 17, 1998

Abstract: The negatively charged phosphodiester linkages in DNA {-O(PO_2^-)O-} have been replaced by a novel methylthiourea {-NHC(=SMe^+)NH-} backbone. The backbone is positively charged, achiral, and stable and can be easily synthesized. A basic strategy for the synthesis of deoxynucleic methylthioureas (DNmt) is described. Synthetic procedures are provided for thymidyl DNmts (1−4 linkages). Synthesis proceeds in 3′−5′ direction and involves coupling of a protected 3′-isothiocyanate with the corresponding 5′-amine of the growing oligo chain. Coupling reactions at room temperature are nearly quantitative, and products are easily purified. The method of continuous variation indicates that there is an equilibrium complex with a molar ratio of d(Tmt) to r(Ap) or d(Ap) of 2:1. Continuous variation plots carried out at temperatures from 15 to 60 °C show a triple helical complex. Titration scans over the entire range of wavelengths (240−285 nm) confirm binding in triple helical fashion. Thermal denaturation analyses show pronounced hysteresis with poly(dA) as well as poly(rA). Hysteresis is more pronounced at higher ionic strengths due to a slower annealing process. DNmt shows fidelity in binding to polynucleotides as there is little hyperchromicity observed in denaturation of DNmt complexes to noncomplementary deoxynucleotides and ribonucleotides. The effect of ionic strength on thermal denaturation is very pronounced, with stability greatest at low ionic strengths. Thermal denaturation studies show melting points of >15 °C per base pair in complexes of DNmt with poly(dA) and poly(rA).

Introduction

Antisense oligos with various backbone modifications[1−4] have attracted considerable attention. The negatively charged phosphodiester linkages of double- and triple-stranded DNA and RNA reside side by side causing considerable charge−charge electrostatic repulsion. This is particularly so at low (physiological) ionic strength. This feature, as well as the susceptibility of DNA and RNA to nuclease activity, limits the usefulness of RNA and DNA as antisense or antigene drugs.[5−8] Among other requirements, successful development of antisense therapeutics presupposes[9,10] the oligos to (a) be stable in vivo, (b) have improved permeability and cellular uptake, and (c) have greater binding affinity with high specificity.[11] The desirability of replacing the phosphodiester linkage by other linkages that are either neutral or positively charged and resistant toward nuclease degradation in order to provide more effective antigene/antisense agents has previously been discussed in detail.[8,12,13] Also considered has been the desirability in future studies to modify oligonucleotides in such a manner that cellular uptake is enhanced.[12] We have previously reported the replacement of the phosphate linkages in DNA and RNA by achiral guanido groups that provide a new class of guanidinium (g)-linked nucleosides which we identify as DNG.[14−17] Peptide (PNA-neutral),[18,19] PHONA,[20] methyl phosphonate (DNAmp-neutral),[21,22] phosphorothioate (DNAs-anionic),[12,13,23] phosphoramidate,[24] amido,[25] MMI,[26] boronated oligonucleotides,[27−29]

(1) Bennett, C. F. *Biochem. Pharmacol.* **1998**, *55*, 9.
(2) Alama, A.; Barbieri, F.; Cagnoli, M.; Schettini, G. *Pharmacol. Res.* **1997**, *36*, 171.
(3) Manoharan, M. *Designer Antisense oligonucleotides*: *conjugation chemistry and functionality placement*; CRC Press: Boca Raton, FL, 1993.
(4) Mesmaeker, A. D.; Altmann, K.-H.; Wendeborn, S.; Wolf, R. M. *Pure Appl. Chem.* **1997**, *69*, 437.
(5) Temsamani, J.; Guinot, P. *Biotechnol. Appl. Biochem.* **1997**, *26*, 65.
(6) Uhlmann, E.; Peyman, A. *Chem. Rev.* **1990**, *90*, 543.
(7) Crooke, R. M. *Anticancer Drug Des.* **1991**, *6*, 609.
(8) Crooke, S. T. *Ann. Rev. Pharmacol. Toxicol.* **1992**, *32*, 329.
(9) Miller, P.; Ts'o, P. *Anticancer Drug Des.* **1987**, *2*, 117.
(10) Milligan, J. F.; Matteucci, M. D.; Martin, J. C. *J. Med. Chem.* **1993**, *36*, 1923.
(11) Mesmaeker, A. D.; Altmann, K.-H.; Waldner, A.; Wendeborn, S. *Curr Opin. Struct Biol.* **1995**, 343.
(12) Cook, P. D. In *Antisense Research and Applications*; Lebleu, S. T. C. B., Ed.; CRC Press: Boca Raton, FL, 1993; p 149.
(13) Morvan, F.; Porumb, H.; Degols, G.; Lefebvre, I.; Pompon, A.; Sproat, B. S.; Rayner, B.; Malvy, C.; Lebleu, B.; Imbach, J.-L. *J. Med. Chem.* **1993**, *36*, 280.
(14) Dempcy, R. O.; Almarsson, O.; Bruice, T. C. *Proc. Natl. Acad. Sci. U.S.A.* **1994**, *91*, 7864.
(15) Dempcy, R. O.; Browne, K.; Bruice, T. C. *Proc. Natl. Acad. Sci. U.S.A.* **1995**, *92*.
(16) Dempcy, R. O.; Browne, K.; Bruice, T. C. *J. Am. Chem. Soc.* **1995**, *117*, 6140.
(17) Dempcy, R. O.; Luo, J.; Bruice, T. C. *Proc. Natl. Acad. Sci. U.S.A.* **1996**, *93*, 4326.
(18) Egholm, M.; Buchardt, O.; Nielsen, P. E.; Berg, R. H. *J. Am. Chem. Soc.* **1992**, *114*, 1895.
(19) Nielsen, P. E.; Haaima, G. *Chem. Soc. Rev.* **1997**, 73.
(20) Peyman, A.; Uhlmann, E.; Wagner, K.; Augustin, S.; Breipohl, G.; Will, D. W.; Schafer, A.; Wallmeier, H. *Angew. Chem., Int. Ed. Engl.* **1996**, *35*, 2636.
(21) Stein, C. A.; Cheng, Y.-C. *Science* **1993**, *261*, 1004.
(22) Y.Tseng, B.; Ts'o, P. O. P. *Antisense Res. Dev.* **1995**, *5*, 251.
(23) Marshall, W. S.; Caruthers, M. H. *Science* **1993**, *259*, 1564.
(24) Gryaznov, S.; Chen, J.-K. *J. Am. Chem. Soc.* **1994**, *116*, 3143.
(25) Mesmaeker, A. D.; Lesueur, C.; Bevierre, M.-O.; Waldner, A.; Fritsch, V.; Wolf, R. M. *Angew. Chem., Int. Ed. Engl.* **1996**, *35*, 2790.
(26) Sanghvi, Y. S.; Swayze, E. E.; Peoc'h, D.; Bhat, B.; Dimock, S. *Nucleosides Nucleotides* **1997**, *16*, 907.
(27) Sood, A.; Spielvogel, B.; Shaw, B. *J. Am. Chem. Soc.* **1989**, *111*, 9234.
(28) Sood, A.; Shaw, B.; Spielvogel, B. *J. Am. Chem. Soc.* **1990**, *112*, 9000.
(29) Spielvogel, B.; Sood, A.; Shaw, B.; Hall, I. *Pure Appl. Chem.* **1991**, *63*, 415.

10.1021/ja9829416 CCC: $15.00
Published on Web 11/19/1998

Scheme 1. Structures of Some Backbone-Modified Oligonucleotides

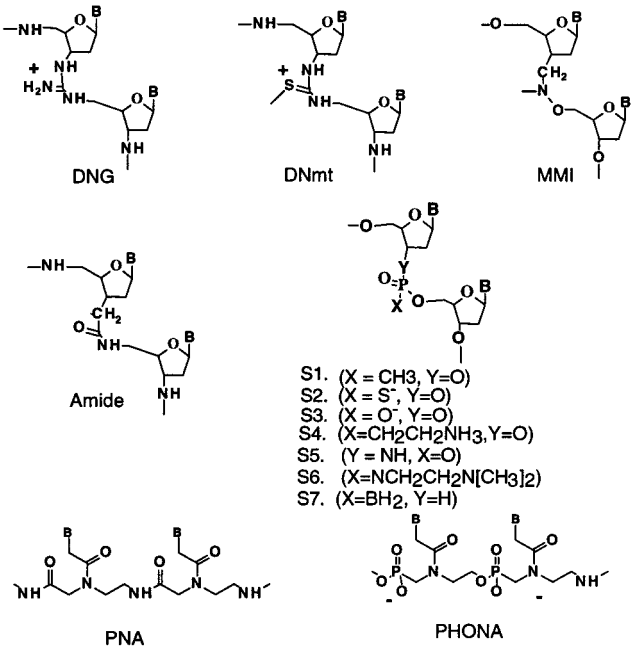

ethylmorpholino and dimethylamino phosphoramidates,[30,31] aminomethyl phosphonates,[32] and guanido (Scheme 1) are, among others,[33−40] some examples of backbone-modified oligos with different electrostatic attractions. Small positively charged oligos (DNG) show unprecedented binding to nucleic acids with retention of specificity.[15,16,41] The nonionic oligo DNAmp exhibits the ability to be transported into cells by passive diffusion/fluid-phase endocytosis and is more resistant to degradation than DNA.[12] Both DNAmp and DNAs, however, have individual limited drawbacks of stereoisomeric complexity,[32] solubility (DNAmp), and toxicity (DNAs).[13,42] These findings have led recently to the development of mixed backbone oligonucleotides (MBOs)[13,42,43] where the phosphorothioates and methyl phosphonates have been alternated in an oligo backbone to produce improved antisense properties. To investigate the effects on binding and specificity of a positively charged backbone with hydrophobicity, we have recently designed the polycationic nucleotide linkage with methylisothiouronium salts,[44] or methylated thioureas,[45] abbreviated as DNmt (Scheme 1). In this publication we report on the synthesis of thymidyl methylthioureas (Tmts) and the nature of equilibrium complexes of pentameric Tmt with poly(dA) and poly(rA).

Materials and Methods

Materials. The concentrations of nucleotide solutions were determined using the extinction coefficients (per mole of nucleotide) calculated according to the nearest neighboring effects.[46] For $d(Tmt)_5$ we used $\epsilon_{268} = 8700\ M^{-1}\ cm^{-1}$. All experiments were conducted in either (a) 0.015 M phosphate buffer (pH 7−7.5) or (b) 0.008 M phosphate buffer (pH 6.85), and the ionic strength, μ, was adjusted with KCl and are presented with the corresponding concentration of KCl. The concentrations of nucleosides, expressed in M/base, were 2.1×10^{-5} to 6.3×10^{-5} M, and the ionic strength $\mu = 0.06-0.6$. The concentration is referred to the limiting component forming the triplex (e.g., a concentration of 2.1×10^{-5} M/base in the reaction of A + 2T means [A] = 2.1×10^{-5} M/base and [T] = 4.2×10^{-5} M/base). All stock solutions were kept at 4 °C between experiments.

Sample Preparation. Five magnetically stirred screw-cap cuvettes of 1-cm path length were used for data collection: four with samples to be measured and one for the temperature monitoring. The measurement chamber was purged continuously with dry nitrogen to prevent condensation of water vapor at lower temperatures. Annealing and melting were followed spectrophotometrically at the given wavelength.

UV Spectroscopy and Data Collection. A Cary 1E UV/vis spectrophotometer equipped with temperature programming and regulation and a thermal melting software package were used for data collection at $\lambda = 260$ nm. Spectrophotometer stability and λ alignment were checked prior to initiation of each melting point experiment. For the T_m determinations hypochromicity was used. Data were recorded every 1.0°. The samples were heated from 25 to 95 °C at 5 deg/min (Scheme 1), the annealing (95−10 °C) and the melting (10−95 °C) were conducted at 0.13 deg/min, and the samples were brought back to 25 °C at a rate of 5 deg/min. The reaction solutions were equilibrated for 15 min at the highest and lowest temperatures.[47]

Synthesis. General Procedures. All reactions were performed under a positive atmosphere of dry nitrogen. ^{1}H NMR spectra were obtained at 400 MHz unless indicated otherwise and ^{13}C NMR spectra at 125 MHz; chemical shifts (δ) are relative to internal TMS, and coupling constants (J) are in hertz. Splitting patterns are designated singlet (s), doublet (d), triplet (t), quartet (q), multiplet (m), or broad (b). IR spectra were taken in KBr pellets using Perkin-Elmer 1300 spectrophotometer. TLC was carried out on silica gel (kieselgel 60 F_{254}) and 0.25-mm coated commercial silica plates and visualized by UV light or *p*-anisaldehyde in ethanol/sulfuric acid. Flash column chromatography employed E. Merck silica gel (kieselgel 60, 200−400 mesh) as the stationary phase. Individual mobile-phase systems are described in the Experimental Section. *TtT* refers to thymidyl dinucleotide with a thiourea linkage, *TmtT* refers to a thymidyl dinucleotide with a methylated thiourea linkage.

3′-Isothiocyanato-5′-*O*-trityl-3′-deoxythymidine (4). To a solution of 300 mg (0.6192 mmol) of 3′-amino-5′-*O*-tritydeoxythymidine in 20 mL of dichloromethane was added 150 mg (0.64 mmol) of thiocarbonylpyridone, and the resulting solution was stirred at room temperature for 6 h. TLC analysis in 80% EtOAc:20% hexanes shows complete disappearance of the amine ($R_f = 0.1$). The product has a R_f value of 0.8 and pyridone of 0.45. The solvent was rotovaporated and the product chromatographed in EtOAC:hexanes (1:1) to give 290 mg of the product (88%). ^{1}H NMR (200 MHz, $CDCl_3$): δ 9.636 (1H, s, NH), 7.493 (1H, s, 6-H), 7.493−7.279 (15H, m, trityl-H), 6.2899 (1H, t, J = 6.18 Hz, 1′-H), 4.606 (1H, q, J = 7.32 Hz, 1.82 Hz, 3′-H), 4.139 (1H, q, J = 7.32 Hz, 5.12 Hz, 4′-H), 3.60 (1H, dd, J = 8.18 Hz,

(30) Jung, P. M.; Letsinger, R. L.; Histand, G. *Nucleosides Nucleotides* **1994**, *13*, 1597.
(31) Letsinger, R. L.; Singman, C. N.; Histand, G.; Salunkhe, M. *J. Am. Chem. Soc.* **1988**, *110*, 4470.
(32) Huang, Q.; Syi, J.-L.; Delaney, W.; Cook, A. F. *Bioconjugate Chem.* **1994**, *5*, 47.
(33) Vasseur, J.-J.; Debart, F.; Sanghvi, Y. S.; Cook, P. D. *J. Am. Chem. Soc.* **1992**, *114*, 4006.
(34) Blattler, M. O.; Wenz, C.; Pingoud, A.; Benner, S. A. *J. Am. Chem. Soc.* **1991**, *120*, 2674.
(35) James, K. D.; Kiedrowski, G.v.; Ellington, A. D. *Nucleosides Nucleotides* **1997**, *16*, 1821.
(36) Jones, R. J.; Lin, K.-Y.; Milligan, J. F.; Wadwani, S.; Matteucci, M. D. *J. Org. Chem.* **1993**, *58*, 2983.
(37) Mesmaeker, A. D.; Haner, R.; Martin, P.; Moser, H. *Acc. Chem. Res.* **1995**, *28*, 366.
(38) Rao, T. S.; Jayaraman, K.; Durland, R. H.; Revankar, G. R. *Nucleosides Nucleotides* **1997**, *13*, 255.
(39) Stirchak, E. P.; Summerton, J. E. *J. Org. Chem.* **1987**, *52*, 4202.
(40) Thibon, J.; Latxague, L.; Deleris, G. *J. Org. Chem.* **1997**, *62*, 4635.
(41) Browne, K. A.; Dempcy, R. O.; Bruice, T. C. *Proc. Natl. Acad. Sci. U.S.A.* **1995**, *92*, 7051.
(42) Agrawal, S.; Jiang, Z.; Zhao, Q.; Shaw, D.; Sun, D.; Saxinger, C. *Nucleosides Nucleotides* **1997**, *16*, 927.
(43) Iyer, R. P.; Yu, D.; Jiang, Z.; Agrawal, S. *Tetrahedron* **1996**, *52*, 14419.
(44) Arya, D. P.; Bruice, T. C. *J. Am. Chem. Soc.* **1998**, *120*, 6619.
(45) The methyl isothiouronium salts could be drawn with the positive charge on nitrogen.
(46) Blasko, A.; Dempcy, R. O.; Minyat, E. E.; Bruice, T. C. *J. Am. Chem. Soc.* **1996**, *118*, 7892.
(47) Blasko, A.; Dempcy, R. O.; Minyat, E. E.; Bruice, T. C. *Biochemistry* **1997**, *36*, 7821.

5.12 Hz, 5′-H), 2.858 (2H, m, 2′-H), 1.5612 (3H, s, Me). **δ^{13}C** (d_6-DMSO + $CDCl_3$, 75 MHz): 149.794, 146.854, 142.249, 134.811, 127.558, 127.185, 126.628, 125.812, 109.767, 84.4025, 83.395, 80.2512, 54.410, 11.657. IR (KBr pellet): 3190, 3050 (aromatic C−H), 2083, 2047 (N═C═S), 1689 (C═O), 1458, 1273, 1099, 1063. *m*/**z**: 526.2 (M + H)$^+$. Anal. Calcd: C, 68.6%; H, 5.2%. Found: C, 68.5%; H, 5.3%.

5′-Azido-3′-*O*-trityl-5′-deoxythymidine (2). To a solution of 4 g (14.96 mmol) of 5′-azidodeoxythymidine (**1**) in 100 mL of pyridine was added 50 mg (0.4098 mmol) of (dimethylamino)pyridine followed by 10 g (0.035 mol) of triphenylmethyl chloride. The resulting solution was stirred at 100 °C for 48 h. TLC analysis in EtOAc shows complete disappearance of the starting material (R_f = 0.1). The product has a R_f value of 0.4. The solvent was rotovaporated and the resulting concentrate chromatographed in EtOAC:hexanes (1:1) followed by elution with 100% EtOAc to give 7 g of the product (91.9 %). ^{1}H NMR (400 MHz, $CDCl_3$): δ 8.651 (1H, s, NH), 7.90−7.25 (15H, m, trityl-H), 7.173 (1H, d, J = 1.2 Hz, 6-H), 6.33 (1H, q, J = 5.6 Hz, 3.6 Hz, 1′-H), 4.226 (1H, h, J = 5.6 Hz, 3.6 Hz, 3.2 Hz, 3′-H), 3.910 (1H, q, J = 3.2 Hz, 2.8 Hz, 4′-H), 3.329 (1H, dd, J = 9.6 Hz, 2.8 Hz, 5′-H), 2.740 (1H, dd, J = 9.6 Hz, 3.2 Hz, 5′-H), 1.990 (1H, m, 2′-H), 1.860 (3H, d, J = 1.2 Hz, Me), 1.699 (2H, m, 2′-H). δ^{13}C ($CDCl_3$, 125 MHz): 163.209, 150.055, 146.777, 134.474, 128. 885, 128.048, 127. 479, 111.245, 87.933, 84.549, 52.134, 39.079, 12.520. IR (KBr pellet): 3051 (aromatic C−H), 2928 (aliphatic C−H), 2099 (N═N═N), 1686 (C═O), 1481, 1442, 1274, 1029. *m*/*z*: FAB: 510 (M + H)$^+$. Anal. Calcd: C, 71.4%; H, 6.0%. Found: C, 71.56%; H, 6.05%.

5′-Amino-3′-*O*-trityl-5′-deoxythymidine (3). To a solution of 1.5 g (2.94 mmol) of 5′-azido-3′-*O*-trityl-5′-deoxythymidine (**2**) in 100 mL of ethanol was added 50 mg of palladium on carbon catalyst (10%). The resulting solution was hydrogenated at 45 psi for 1 h. TLC analysis in EtOAc showed complete disappearance of the starting material (R_f = 0.4). The product has a R_f value of 0.1. The solution was filtered over Celite and the solvent evaporated under pressure. Chromatography in 15% MeOH:85% EtOAc gave 1.1 g of the pure product (77.4%). ^{1}H NMR (400 MHz, d_6-DMSO): δ 7.646 (1H, d, J = 1.2 Hz, NH), 7.446−7.264 (15H, m, trityl-H), 6.121 (1H, q, J = 5.2 Hz, 4.0 Hz, 1′-H), 4.20 (1H, d, J = 5.6 Hz, 2′-H), 3.782 (1H, p, J = 5.2 Hz, 3.2 Hz, 4′-H), 3.347 (2H, br, NH_2), 2.455 (1H, dd, J = 4.8 Hz, 5.2 Hz, 5′-H), 2.359 (1H, dd, J = 4.8 Hz, 5.2 Hz, 5′-H), 1.719 (3H, d, J = 1.2 Hz, Me), 1.410 (1H, d, J = 5.6 Hz, 2′-H), 1.380 (1H, d, J = 6 Hz, 2′-H). δ^{13}C (d_6-DMSO, 125 MHz): 163.573, 150.419, 144.198, 136.111, 128.510, 128.047, 127.266, 109.620, 87.058, 86.527, 83.561, 74.882, 43.179, 37.520, 12.083. IR (KBr pellet): 3388, 3310 (N−H), 3054 (aromatic C−H), 2948, 2917 (aliphatic C−H), 1655 (C═O), 1447, 1273, 1023. *m*/*z*: 484 (M + H)$^+$. HRMS (FAB): 484.22312, calcd for $C_{29}H_{30}N_3O_4$ 484.22363.

5′-*O*-Trityl-TtT-3′-*O*-trityl (5). To a solution of 250 mg (0.474 mmol) of 3′-isothiocyanate-5′-*O*-trityl-3′-deoxythymidine (**4**) in 20 mL of anhydrous acetonitrile was added 240 mg (0.496 mmol) of 5′-amino-3′-*O*-trityl-5′-deoxythymidine (**3**) followed by 5 mg of (dimethylamino)-pyridine, and the resulting solution was stirred at room temperature. A white precipitate began to appear after 20 min. The reaction was stirred for 2 h and the solution then cooled to 0 °C for 30 min. The white precipitate was then collected by filtration, washed with cold ether, and dried to give 460 mg (96.2%) of analytically pure product. TLC analysis in EtOAc showed complete disappearance of the amine (R_f = 0.1). The product has a R_f value of 0.4, and the isothiocyanate has a R_f value of 0.85. ^{1}H NMR (400 MHz, $CDCl_3$): δ 10.371 (1H, s, NH), 10.229 (1H, s, NH), 10.135 (1H, s, NH), 9.990 (1H, s, NH), 7.606 (1H, s 6-H), 7.450−7.233 (30H, m, trityl-H), 6.932 (1H, s, 6-H), 6.537 (1H, t, J = 6.8 Hz, 1′-H), 5.989 (1H, t, J = 6.8 Hz, 1′-H), 5.237 (1H, b, 3′-H), 4.287 (1H, b, 3′-H), 4.146 (1H, m, 4′-H), 3.790 (1H, m, 4′-H), 3.65 (2H, d, J = 9.2 Hz, 2′-H), 3.345 (2H, d, J = 9.2 Hz, 5′-H), 2.489−2.334 (4H, m, 2′-H), 1.804 (3H, s, Me), 1.392 (3H, s, Me). δ^{13}C ($CDCl_3$, 125 MHz): 173.526, 164.332, 164.036, 151.064, 150.926, 150.608, 146.785, 143.758, 143.364, 128.639, 128.101, 127.941, 127.828, 127.433, 127.213, 127.152, 111.745, 111.199, 87.910, 87.478, 85.680, 84.360, 75.097, 64.803, 55.556, 36.750, 12.240, 11.640. IR (KBr pellet): 3395, 3451 (N−H), 3361, 3317 (N−H), 3050 (aromatic C−H), 1692 (C═O), 1535, 1447, 1267, 1053. *m*/*z*: 1009.18 (M + H)$^+$. Anal. Calcd: C, 70.2%; H, 5.6%. Found: C, 70.3%; H, 5.55%.

5′-OH-TmtT-3′-OH (6). To a solution of 30 mg (0.029 mmol) of 5′-*O*-trityl-TtT-3′-*O*-trityl (**5**) in 20 mL of ethanol was added 10 mL of methyl iodide, and the resulting solution was stirred at room temperature for 2 h, followed by heating to 35 °C for 20 min. TLC analysis in EtOAc showed complete disappearance of the starting material (R_f = 0.6). The product has a R_f value of 0.5. The solvents were then evaporated under pressure, and the residue was washed with hexanes and dried to give 29 mg of a 5′-*O*-trityl-TmtT-3′-*O*-trityl as a yellowish solid (97.6%). *m*/*z*: 1024 (M + H)$^+$. HRMS (FAB): 1023.4103.

To a solution of 20 mg (0.0195 mmol) of 5′-*O*-trityl-Tmt-T-3′-*O*-trityl in 10 mL of dichloromethane was added 10 mL of trifluoroacetic acid. The resulting solution was stirred at room temperature for 1 h. The solvents were then evaporated under pressure, and to the resulting gel was added 100 mL of diethyl ether. The white precipitate obtained was filtered off and washed with ether and dichloromethane to give 9 mg of dry product (85.7%). ^{1}H NMR (400 MHz, d_6-DMSO): δ 11.56 (2H, NH), 9.677 (1H, br, NH), 9.33 (1H, d, J = 6.8 Hz), 9.210 (1H, br, NH), 7.914 (1H, s, 6-H), 7.688 (1H, s, 6-H), 6.452 (1H, t, J = 6.8 Hz, 1′-H), 6.336 (1H, t, J = 6.8 Hz, 1′-H), 5.661 (2H, br, OH), 4.681 (1H, br, 3′-H), 4.494 (1H, m, 3′-H), 4.292−4.054 (2H, m, 4′-H), 3.989−3.60 (4H, m, 5′-H), 2.904 (3H, s, Me), 2.715 (2H, m, 2′-H), 2.34 (2H, m, 2′-H), 2.00 (3H, s, Me). δ^{13}C (d_6-DMSO, 125 MHz): 168.101, 163.618, 163.375, 150.319, 150.266, 136.649, 136.140, 109.816, 109.490, 83.810, 83.408, 82.915, 70.398, 60.134, 54.717, 53.837, 46.752, 44.855, 37.640, 36.525, 14.844, 14.184. IR (KBr pellet): 3465 (O−H), 3385, 3451 (N−H), 3044 (aromatic C−H), 2959 (aliphatic C−H), 1682 (C═O), 1545, 1457, 1267, 1063. *m*/*z*: 539 (M + H)$^+$. HRMS (FAB): 539.1933, calcd for $C_{22}H_{31}N_6O_8S$ 539.19240.

5′-N-MmTr-TtT-3′-OH (9a). To a solution of 100 mg (0.180 mmol) of 3′-isothiocyanato-5′-N-MmTr-3′,5′-dideoxythymidine (**7**) in 10 mL of anhydrous pyridine was added 100 mg (0.414 mmol) of 5′-amino-5′-deoxythymidine (**8**) followed by 5 mg of (dimethylamino)pyridine, and the resulting solution was stirred at room temperature for 2 h. Pyridine was evaporated under pressure, and 20 mL of water was added to the residue to precipitate the product. The product was extracted into 2 × 30 mL of chloroform, washed successively with water to remove the excess amine. The organic extracts are dried over sodium sulfate and evaporated to give 130 mg of a dry product (90.9%). ^{1}H NMR (400 MHz, d_6-DMSO): δ 10.596 (1H, s, NH), 10.550 (1H, s, NH), 7.735 (2H, NH), 7.120 (4H, d J = 7.6 Hz, trityl-H), 7.01 (2H, d, J = 9.2 Hz, trityl-H), 6.89 (4H, t, J = 7.6 Hz, trityl-H), 6.819 (2H, m, trityl-H), 6.437 (2H, d, J = 9.2 Hz, trityl-H), 5.88 (2H, m, 1′-H), 4.734 (2H, d, J = 4.4 Hz), 3.897 (1H, m), 3.560 (2H, m), 3.407 (3H, s, OMe), 2.89 (1H, s), 2.22 (3H, m). 1.911 (3H, m), 1.669 (1H, s), 1.528 (3H, s, Me), 1.416 (3H, s, Me). δ^{13}C ($CDCl_3$, 125 MHz): 171.136, 164.460, 157.762, 150.988, 149.577, 145.913, 140.549, 137.758, 136.043, 129.754, 128.480, 127.744,126.242, 123.731, 113.065, 111.510, 84.716, 77.206, 70.144, 55.101, 45.732, 38.115, 20.986, 12.452. IR (KBr pellet): 3467 (O−H), 3285, 3248 (N−H), 3070 (aromatic C−H), 2950 (aliphatic C−H), 2328, 1683 (C═O), 1545, 1457, 1267, 1063. *m*/*z*: FAB 796 (M + H)$^+$. Anal. Calcd: C, 61.9%; H, 5.7%. Found: C, 62%; H, 5.68%.

5′-NH_3^+-TtT-3′-OH (10a). To a solution of 120 mg (0.150 mmol) of 5′-N-MmTr-TtT-3′-OH (**9a**) in 20 mL of chloroform was added 10 mL of acetic acid. The resulting solution was stirred at room temperature for 4 h. TLC analysis in BuOH:CH_3COOH:H_2O (5:2:3) shows complete disappearance of the starting material (R_f = 0.8). The product has a R_f value of 0.4. The solvents were then evaporated under pressure, and to the resulting gel was added 100 mL of diethyl ether. The white precipitate obtained was centrifuged and washed with diethyl ether and dichloromethane to give 75 mg of dry product (94.9%). ^{1}H NMR (400 MHz, d_4-MeOD): δ 7.350 (1H, s, NH), 7.331 (1H, s, NH), 7.081 (2H, d, J = 1.2 Hz, 6-H), 6.063 (1H, t, J = 7.2 Hz, 1′-H), 5.955 (1H, t, J = 6.4 Hz, 1′-H), 4.185 (2H, m, 3′-H), 3.88 (3H, m), 3.676 (3H, s, br, NH_3^+), 3.368 (1H, d, J = 3.2 Hz), 3.327 (1H, d, J = 3.2 Hz), 3.157 (2H, m), 2.480 (1H, br, OH), 2.235 (1H, m), 2.105 (2H, m), 1.779 (3H, s, CH_3CO_2-), 1.744 (3H, d, J = 1.2 Hz, Me), 1.733 (3H, d, J = 1.2 Hz, Me). δ^{13}C (d_4-MeOD, 125 MHz): 178.892, 166.405, 152.416, 152.340, 139.588, 138.245, 112.012, 111.944, 88.487, 86.796, 86.363, 82.676, 73.019, 56.519, 42.887, 39.905, 36.810, 23.276, 12.944, 12.648,

12.466. IR (KBr pellet): 3500−2700 (O−H, N−H + C−H), 2342, 1688 (C═O), 1545, 1459, 1267, 1060. *m/z*: FAB, 525 $(M + H)^+$.

5′-N-MmTr-TtTtTtTtT-3′-OH (9d). To a solution of 120 mg (0.088 mmol) of 5′-N-MmTr-TtTtTtT-3′-OH (**9c**) in 20 mL of chloroform was added 10 mL of acetic acid. The resulting solution was stirred at room temperature for 4 h. TLC analysis in $BuOH:CH_3COOH:H_2O$ (5:2:3) showed complete disappearance of the starting material ($R_f = 0.6$). The product has a R_f value of 0.35. The solvents were then evaporated under pressure, and to the resulting gel was added 100 mL of diethyl ether. The white precipitate obtained was centrifuged and washed with diethyl ether (2 × 15 mL) and dichloromethane (2 × 15 mL) to give 100.5 mg of dry product (**10c**, 99.5%). *m/z*: 1089.20 $(M + H)^+$.

To a solution of 105 mg (0.189 mmol) of 3′-isothiocyanato-5′-N-MmTr-3′,5′-dideoxythymidine (**7**) in 10 mL of anhydrous pyridine was added 95 mg (0.0827 mmol) of 5′-NH_3^+-TtTtTtTtT-3′-OH (**10c**) followed by 25 mg of (dimethylamino)pyridine, and the resulting solution was stirred at room temperature for 6 h. Pyridine was evaporated under pressure and the residue washed with 2 × 20 mL of chloroform to precipitate the product and remove any unreacted isothiocyanate. TLC analysis in $BuOH:CH_3COOH:H_2O$ (5:2:3) showed complete disappearance of the amine ($R_f = 0.35$). The product has a R_f value of 0.65. The white product obtained was filtered off, washed with 2 × 10 mL of water, and dried to give 129 mg of product (95.5%). ^{1}H NMR (400 MHz, d_6-DMSO): 11.351 (5H, br, NH), 8.126 (1H, s, 6-H), 8.114 (1H, s, 6-H), 8.048 (1H, br, NH), 7.667 (2H, br, NH), 7.543 (2H, br, 6-H), 7.479 (1H, s, 6-H), 7.39 (4H, d, $J = 5.6$ Hz, trityl-H), 7.259 (4H, m, trityl-H), 7.154 (2H, d, $J = 5.6$ Hz, trityl-H), 6.81 (2H, d, $J = 6.8$ Hz, trityl-H), 6.68 (2H, d, $J = 5.6$ Hz, trityl-H), 6.16 (5H, m, 1′-H), 4.707 (3H, m), 4.19−3.82 (12H, m), 3.70 (3H, OMe), 3.684 (2H, s), 3.567 (2H, br), 2.998 (5H, s), 2.372 (5H, m), 2.139 (5H, m), 1.9 (1H, s), 1.807 (6H, s, Me), 1.79 (3H, s, Me), 1.759 (3H, s, Me), 1.705 (3H, s, Me). δ^{13}C (d_6-DMSO, 125 MHz): 182.684, 172.218, 170.048, 163.767, 157.420, 154.863, 150.690, 150.530, 150.483, 149.631, 146.273, 137.771, 137.581, 137.042, 136.117, 135.997, 135.895, 129.650, 128.303, 127.742, 126.125, 123.959, 113.049, 110.001, 109.950, 109.564, 107.682, 106.786, 84.439, 83.612, 83.077, 82.672, 82.268, 81.675, 80.746, 79.210, 74.570, 71.286, 69.725, 55.395, 54.983, 54.142, 46.801, 44.784, 38.936, 38.306, 36.780, 36.343, 35.258, 21.198, 20.867, 12.499, 12.313, 12.233, 12.193. IR (KBr pellet): 3464 (O−H), 3288, 3228 (N−H), 3060 (aromatic C−H), 2943 (aliphatic C−H), 1689 (C═O), 1542, 1455, 1266, 1063. *m/z*: FAB, 1643 $(M + H)^+$. Anal. Calcd: C, 54.1%; H, 5.3%. Found: C, 53.96%; H, 5.17%.

5′-NH_3^+-TmtTmtTmtTmtT-3′-OH (11d). To a solution of 20 mg (0.012 mmol) of 5′-N-MmTr-TtTtTtTtT-3′-OH (**9d**) in 3 mL of dimethylformamide was added 5 mL of ethanol and 20 mL of methyl iodide. The resulting solution was stirred at 40 °C for 5 h. The solvents were then evaporated under pressure, and to the resulting gel was added 20 mL of acetic acid and stirred for another 2 h. Acetic acid was then evaporated off and the glue-like residue dissolved in methanol and precipitated with ether. The precipitate was collected by centrifugation and reprecipitated from methanol−ether to give 19 mg of a yellowish product (90.47%). The product was then purified on a preparative Alltech WCX cation exchange column employing 1.50 M ammonium acetate buffer (pH 7.0) as the mobile phase. The purity of the sample was further confirmed by running it on an analytical cation exchange column with 1 M guanidine-HCl as the eluant. The HPLC chromatogram of compound **11d** is shown in the Supporting Information and has a retention time of 18 min, consistent with the presence of five positive charges. IR (KBr pellet): 3275, 3239 (N−H), 3060 (aromatic C−H), 2948 (aliphatic C−H), 1690 (C═O), 1542, 1455, 1264, 1063. *m/z*: (FAB) 1427 $(M + H)^+$, (ESI) 1427.4 $(M + H)^+$, 714.3 $(M + 2H)^{2+}$, $\lambda_{max} = 266.7$ nm.

Results and Discussion

Synthesis. Initial studies were focused on attempts to synthesize (Scheme 3) dimeric thymidyl methylthiourea **6**. Coupling conditions for the formation of the thiourea linkage were optimized using compounds **3** and **4**. The isothiocyanate **4** was easily synthesized by reaction of the corresponding 3′-amino-5′-*O*-trityldideoxythymidine with thiopyridone at room temperature. Compound **3** on the other hand was synthesized in a two-step process from 5′-azido thymidine. Protection of the 3′-hydroxyl with triphenylmethyl chloride in pyridine followed by reduction of the azide gave compound **3** in excellent yields. Protection of 3′-hydroxyl with base labile groups (phenoxyacetyl) led mostly to the rearrangement involving nucleophilic attack by the 5′-amine.

Scheme 2

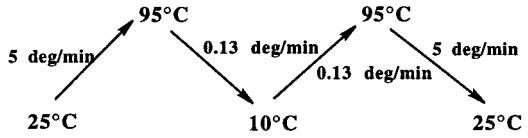

Scheme 3. Synthesis of Dimeric Thymidyl Methylthiourea **6**

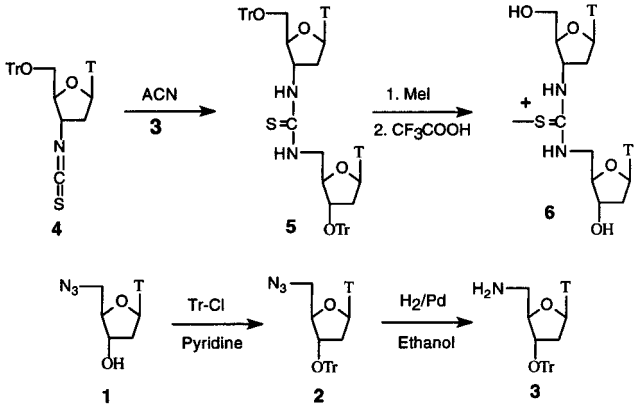

The reaction of **3** with **4** was followed under varying temperatures and solvents to optimize coupling reaction conditions. Heating the isothiocyanates to speed up the reaction led to slight decomposition of the isothiocyanate (reaction with traces of moisture). The reaction proceeds to completion at room temperature in a few hours with pyridine and acetonitrile as the solvents of choice. Thiourea **5** was methylated with excess methyl iodide and the product detritylated with TFA to give DNmt dimer **6**. Compound **6** was found to be analytically pure by HPLC, NMR, and MS. The ^{1}H NMR (1D and 2D) spectrum of compound **6** is shown in the Supporting Information and shows the resolution of similar protons in the two sugar rings. The methyl peak of the thiourea is considerably deshielded and appears at 3 ppm. While the assignments can be easily made in a dimer, longer sequences show much greater overlap and the compounds were then characterized by a combination of NMR, MS, IR, and elemental analysis, and, in the case of methylated thioureas, cation exchange HPLC, MS, and UV analysis.

To extend the synthesis to the formation of polymeric DNmt, attempts were initially made to protect the 3′-hydroxyl with a base labile protecting group so that the 3′−5′ chain extension could (a) be carried out by deprotection of the acid labile trityl group, (b) improve the solubility of monomer **8** and thioureas in organic solvents, and (c) eliminate any possibility of reaction between the 3′-hydroxyl and the 3′-isothiocyanate **7**. Since initial attempts (see discussion above) to carry out that transformation were unsuccessful, anhydrous pyridine was used as a solvent to couple 5′-aminodeoxythymidine **8** with 5′-*N*-Mm-trityl-3′-isothiocyanato-dideoxythymidine. The reaction proceeds to completion in few hours, and the 3′-OH has no reactivity with the isothiocyanate. The lack of a protecting group at the 3′-OH turned out to be a blessing in disguise because of the ease in purification of polymeric thioureas that resulted from it. While 5′-*N*-tritylated thioureas are soluble in some organic solvents, the detritylated amines are easily precipitated on addition of

Scheme 4. Synthesis Plan for T5-mt (**11d**)

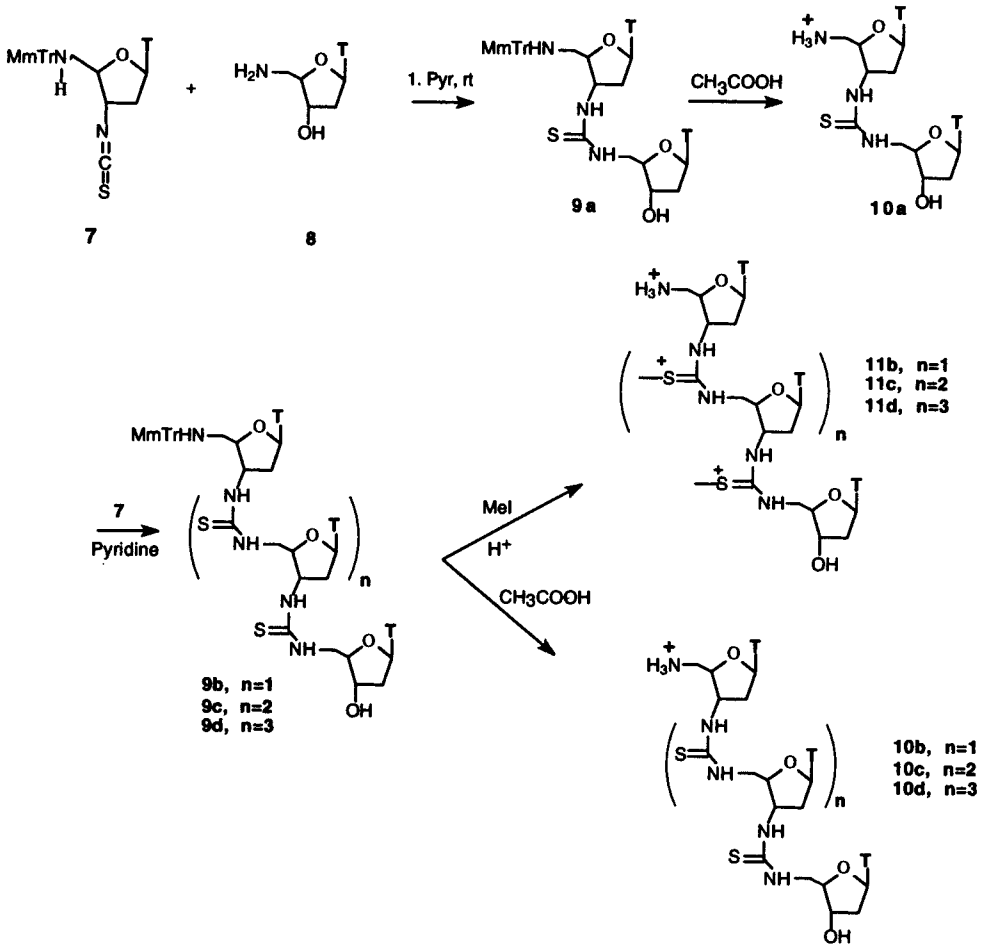

chloroform or ether, making the whole purification process rather trivial (see the Experimental Section).

The synthesis of **11d** (Scheme 4) was then accomplished via a cyclic process starting with a condensation reaction between 3′-isothiocyanato-5′-*N*-Mm-trityl-3′,5′-deoxythymidine (**7**) and 5′-amino-5′-deoxythymidine (**8**), affording the 3′→5′ thiourea-linked dimer **9**. The synthesis of **7** was carried out by protection of 5′-amino-3′-azido-3,′5′-dideoxythymidine[14,15] with monomethoxytrityl chloride followed by hydrogenation of the azido group. The reaction of the resulting 3′-amino-5′-*N*-Mm-trityl-3′,5′-deoxythymidine with excess thiopyridone[48] at room temperature followed by flash chromatography gave compound **7** in 65% overall yield. Chain extension from the dimer followed a cyclic two-step process involving deprotection of the 5′-amino group with acetic acid. The resulting amine was then allowed to condense, in near quantitative yields, with another equivalent of **7** in pyridine for 4−8 h, depending upon the length of the oligomer. 4-(Dimethylamino)pyridine was added in 5−10% molar quantities to speed up the reaction. The thiourea-linked thymidyl oligomers **10b**−**d** were successfully converted to compounds **11b**−**d** by methylation of the thiourea linkages to methylisothiouronium salts in excess methyl iodide. The reaction can be carried out at room temperature or heated to 40 °C, if necessary. Excess heating for over 4 h, however, results in partial methylation of the 3′-OH. Deprotection of methylated polymers with acetic acid was followed by a purification on a preparative Alltech WCX cation exchange column employing 1.50 M ammonium acetate buffer (pH 6−7.0) as the mobile phase. The purity of the sample was further confirmed by passing it through an analytical cation exchange column with 1 M guanidine-HCl as the eluant. The HPLC chromatograms of compounds **11a**−**d** are shown in the Supporting Information. The compounds **11b**, **11c**, and **11d** have retention times of 9.8, 14, and 18 min, respectively, consistent with the presence of three, four, and five positive charges.

Equilibrium Complexes of Thymidyl DNmt with Poly(adenylic) Nucleic Acids. To investigate the interaction of **11d** {5′-NH_3^+-T_{mt}-$(T_{mt})_4$-OH} with polynucleotides, we constructed UV continuous variation plots at different ionic strengths (μ), wavelengths, and temperatures. The method of continuous variation is based on the assumption that the decrease in absorbance is proportional to the number of base pairs hydrogen bonded between the interacting species. Mixtures of **11d** with poly(rA) at 30 °C (Figure 1) reach a minimum absorbance at a mole fraction of ∼0.66 d(Tmt) to 0.34 r(Ap) (single phosphate-linked riboadenosyl unit). These numbers indicate that triple-stranded complexes are formed containing two d(Tmt) for every r(Ap). The same results are obtained at 202 and 280 nm. The absorbance change was much larger and the intersection of lines much easier to define at 202 nm. At 15 °C and 60 °C the plots (see the Supporting Information) have a minima at 0.67 mol % of d(Tmt) at all three wavelengths. This confirms the stable triple helical nature of the DNmt·RNA complex suggested by the lack of hyperchromic shifts in the thermal denaturation studies from 15 to 60 °C.

The plot for **11d** with poly(dA) at 30 °C is also centered near a mole fraction of 0.67 d(Tmt) to 0.33 d(Ap) (Figure 1).

(48) Kim, S.; Yi, K. Y. *J. Org. Chem.* **1986**, *51*, 2613.

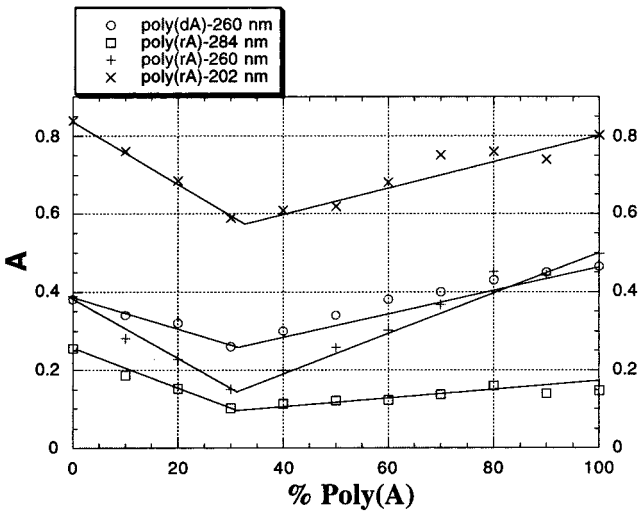

Figure 1. Job plots of poly(rA) (5.3×10^{-5} M), poly(dA) (5.3×10^{-5} M), and **11d** in 15 mM K_2HPO_4 and 0.15 M KCl (pH 7.5) at 30 °C.

Unlike the mixing curves with r(Ap), these curves are much shallower, as the percent hypochromicity is much lower in binding to polydeoxynucleotides. Equilibrium complexes are the same from 30 to 60 °C (data not shown) and confirm the stable triple helical nature of the complexes that DNmt forms with polydeoxyadenosyl nucleotides. Although these results establish that the three-stranded complexes d(Tmt)$_2$·r(Ap) and d(Tmt)$_2$·r(Ap) form under these conditions, they do not specify the composition of equimolar mixtures of d(Tmt) with r(Ap) and d(Ap).[49] In particular, one cannot determine from these results whether two-stranded d(Tmt)·r(Ap) is present in equimolar mixtures or whether the equilibrium products are always d(Tmt)$_2$·r(Ap) and free rA polymer. Continuous variation experiments were carried out with the measurement of complete spectra of each of the different mixtures (Figure 2).[50] Figure 2 shows that, as more of d(Tmt) is being added (decreasing % of polyrA), there is a lowering of absorbance at almost all wavelengths.

Mixing curves with 0 to 50% Tmt are hypochromic at all wavelengths between 235 and 285 nm and curves at any wavelength, where a spectral change occurs, consist of two intersecting straight lines with a single minimum at 66% Tmt residues. The hypochromicity in wavelengths greater than 280 nm is more pronounced at 15 °C as opposed to 60 °C. Since it is unlikely that d(Tmt)·rA has the same absorbency per nucleotide over this entire spectral range as the mixture rA + rA·d(Tmt)$_2$, it is logical to conclude that a 1:1 complex does not exist in appreciable amounts in solutions under these experimental conditions and that the sole complex is rA·d(Tmt)$_2$. Although it may not be very clear from the scale of the titration scans (Figure 2), there are two isosbestic points for d(Tmt) and poly(rA) mixtures. The first occurs at 287.4 nm in 0−66% d(Tmt) mixtures (Figure 3) due to an equivalence of extinction coefficients for rA and rA·d(Tmt)$_2$; the second occurs at 296 nm in 67−100% d(Tmt) and is due to an equivalence of extinction coefficients for d(Tmt) and rA·d(Tmt)$_2$.

(49) It is well-known that the formation of AT2 and AU2 complexes leads to a hypochromic shift at 280 nm, whereas formation of AT and AU complexes does not. Thus A:T is isochromic at this wavelength with respect to A + T, and mixing curves carried out at 280 nm show no hypochromism (see ref 50).

(50) Riley, M.; Maling, B.; Chamberlin, M. J. *J. Mol. Biol.* **1966**, *20*, 359.

Thermal Denaturation Studies. Annealing and melting curves of complexes formed from **11d** {5′-NH_3^+-T_{mt}-$(T_{mt})_4$-OH} with DNA/RNA homooligomers exhibit hysteresis (Figure 4) at the rate of heating−cooling employed (0.13 deg/min). Rates of heating and cooling of up to 0.5 deg/min are generally slow enough to ensure attainment of the equilibrium in the case of duplex to coil transitions in oligonucleotides, i.e., heating and cooling curves coincide.[47] The melting and annealing behavior of DNmt complexes with poly(rA) and poly(dA) was studied at different ionic strengths (μ) at a rate of 0.13 deg/min. At low μ the hysteresis observed is abnormally large. Examination of Figure 4a reveals the cause of this large hysteresis. The complex rA·d(Tmt)$_2$ continues to melt after reaching the terminal temperature of 95 °C; this leads to an initial apparent increase in absorbance as the temperature descent begins, thus causing the abnormally large hysteresis curve.

With an increase in μ (Figure 4b,c) annealing becomes slower. Denaturation studies at high μ show larger hysteresis because the positive and negative charges are attenuated by added salt. As stated previously, the large hysteresis at lower μ can be attributed to the limitation of melting points measurement to 100 °C. This behavior is clarified on studying the melting behavior (Figure 4d) of d(Tmt)$_5$ with dA-20 (a DNA sequence containing 20 adenosine bases). As shown in Figure 4d, the complex shows an ideal hysteresis curve as the triplex melting is now well below 90 °C and the hysteresis observed at low μ is an accurate indication of the melting and annealing processes of DNmt with polynucleotides. In support of these observations is the fact that after thermal melting in a solution containing 0.03 M KCl, reformation of the d(Tmt)$_2$·poly(dA) complex is very slow. The melting mixture does not return to its original absorbency even after standing for 36 h at room temperature. The return to original absorbency is even slower at higher ionic strengths. There is a μ above which the melting transitions for **11d** complexes with poly(rA) and poly(dA) cannot be observed or are too shallow to be accurate representations of a melting point. Increasing the concentrations of the respective strands does however show better transitions at these ionic strengths.

Fidelity in Binding to Polynucleotides. In the thermal denaturation analysis of **11d** {5′-NH_3^+-T_{mt}-$(T_{mt})_4$-OH} bound to poly(dA) (Figure 5a), plots of absorbance at 260 nm (A_{260}) vs temperature exhibit two distinct inflections (T_m = 35 °C and 65 °C, μ = 0.3). We assign the inflection points in Figure 5a to represent denaturation curves of triple- and double-helical structures of **11d** with ss DNA {**11d**$_2$·poly(dA)} and {**11d**·poly(dA)}. Figure 5a also indicates that, under identical conditions, for solutions which contained **11d** and either poly(dG), poly(dC), or poly(dT), no hyperchromic shift at 260 nm was observed between ca. 5−93 °C. However, in the thermal denaturation analysis of **11d** bound to poly(rA) (Figure 5b), plots of A_{260} vs temperature exhibit only one inflection (T_m = 65 °C at μ = 0.15 and T_m = 85 °C at μ = 0.03), representing the melting points of the triple helical structure {**11d**$_2$·poly(rA)}. As observed with polydeoxynucleotides, no hyperchromic shift at 260 nm was observed between ca. 5 and 93 °C for solutions which contained **11d** and either poly(rG) or poly(rC). There was a hyperchromic shift at <10 °C for the denatuaration of poly(rU) annealed to itself.[41] From these results, DNmt appears to bind with DNA and RNA with specificity in forming hybrid duplex and triplex structures.

Equation 1 (Scheme 5) depicts the annealing process (triplex formation). Rates of formation of triplexes are generally slower than those of duplex formation ($k_2 < k_1$). For example, in studies with RNA·RNA complexes, triplex association rates have been found to be 100 times slower than the duplex association rates.[51]

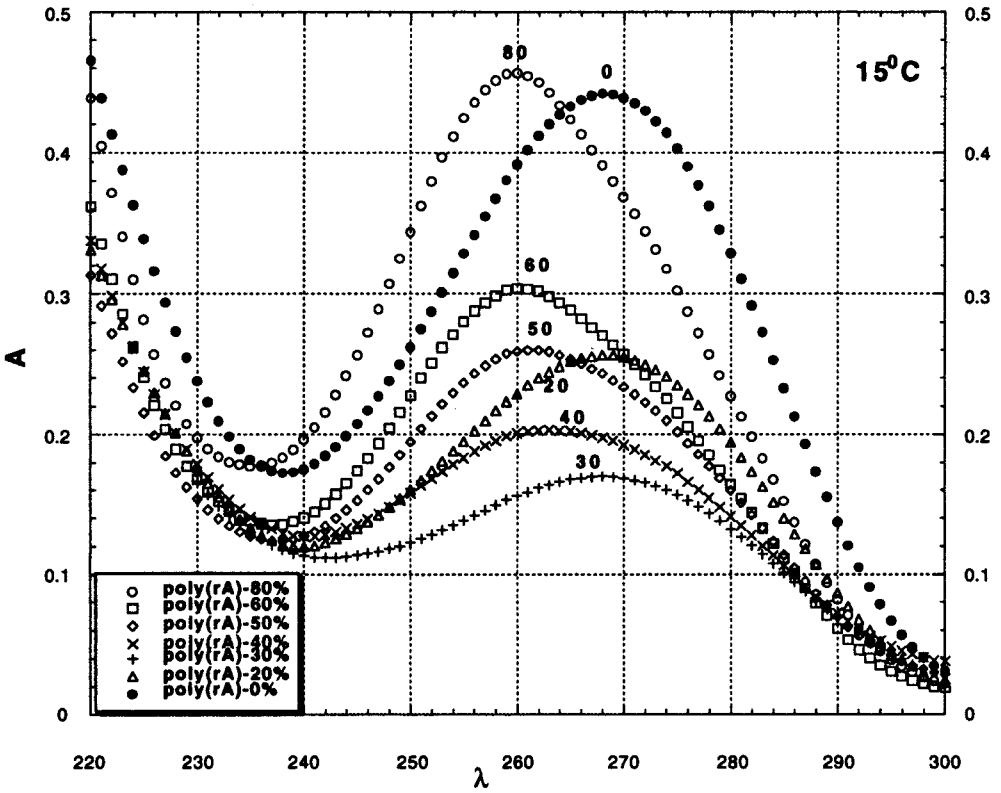

Figure 2. Titration scans of poly(rA) (5.3×10^{-5} M) and **11d** (80% poly(rA) to 0% poly(rA)) in 15 mM K_2HPO_4 and 0.15 M KCl (pH 7.5) at 15 °C.

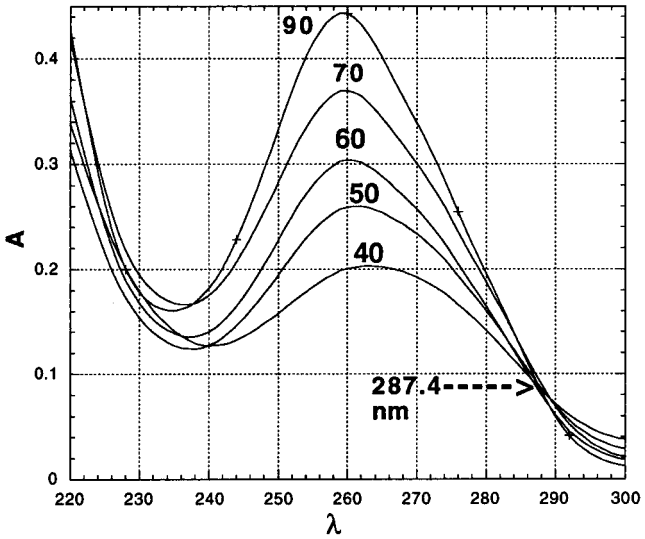

Figure 3. Titration scans of poly(rA) (5.3×10^{-5} M) and **11d** (90% poly(rA) to 40% poly(rA)) in 0.15 mM K_2HPO_4 and 0.15 M KCl (pH 7.5) at 15 °C, showing the inflection point at 287.4 nm.

Electrostatic repulsions between negatively charged phosphates have been suggested as the determining factor in rates of association for RNA and DNA complexes.[52] These electrostatic repulsions become more important in the triplex than in the duplex because the third strand has to come in contact with the duplex that has twice the negative charge of a single strand. Similar rate effects would be expected with DNmt·DNA and DNmt·RNA complexes. The association of Tmt and Ap (eq 1, k_1) is expected to be fast due to attraction of the opposite charges of the backbones. Formation of triplex requires the attraction of a positively charged Tmt to a neutral duplex (Tmt·Ap) and thus is expected to be slower than the first step ($k_2 < k_1$). In the continuous variation plots (annealing, Figures 1 and 2), formation of the triplex as the major species at low temperatures is then due to the thermodynamic stability of the positively charged Tmt·Ap·Tmt complex over the neutral Ap·Tmt duplex. In melting the triplex below 95 °C, one can observe an intermediate duplex at high μ such that $k_2' > k_1'$ (eq 2).

Scheme 5. Triplex Annealing and Melting

$$A_p + T_{mt} \xrightarrow{k_1} A_pT_{mt} \xrightarrow[T_{mt}]{k_2} T_{mt}A_pT_{mt} \quad \text{(low Temp)} \qquad (1)$$

$$T_{mt}A_pT_{mt} \xrightarrow{k_2'} \underset{+\ T_{mt}}{A_pT_{mt}} \xrightarrow{k_1'} A_p + T_{mt} \quad \text{(high Temp)} \qquad (2)$$

Effect of Ionic Strength (μ) on Stability of DNmt·DNA/RNA Complexes. 11d {5′-NH_3^+-T_{mt}-$(T_{mt})_4$-OH} has a significantly greater affinity for poly(dA) and poly(rA) than does thymidyl DNA. As expected, we find that change in μ has an opposite effect on the T_m values of DNmt hybrids with DNA (Figure 6) or RNA as compared to DNA complexes with DNA or RNA. This is due to electrostatic interactions being attenuated by increasing salt concentration. Thus, while DNA·RNA duplexes become more stable with increasing μ, DNmt·RNA complexes become more stable with decrease μ. This is in accord with our previous experience with DNG·RNA complexes. The oppositely charged backbones of the DNmt·RNA complex provide stability. Increase in μ saturates the opposite charges and destabilizes the complex. At any given μ the $d(Tmt)_2$·RNA triplexes are more stable than the $d(Tmt)_2$·DNA triplexes.

The thermal denaturation results have been reduced to the unit of T_m per base pair in order to be able to compare T_m values

(51) Porshke, D.; M, E. *J. Mol. Biol.* **1971**, *30*, 291.
(52) Rougee, M.; Faucon, B.; Mergny, J. L.; Barcelo, F.; Giovannangeli, C.; Garestier, T.; Helene, C. *Biochemistry* **1992**, *31*, 9269.

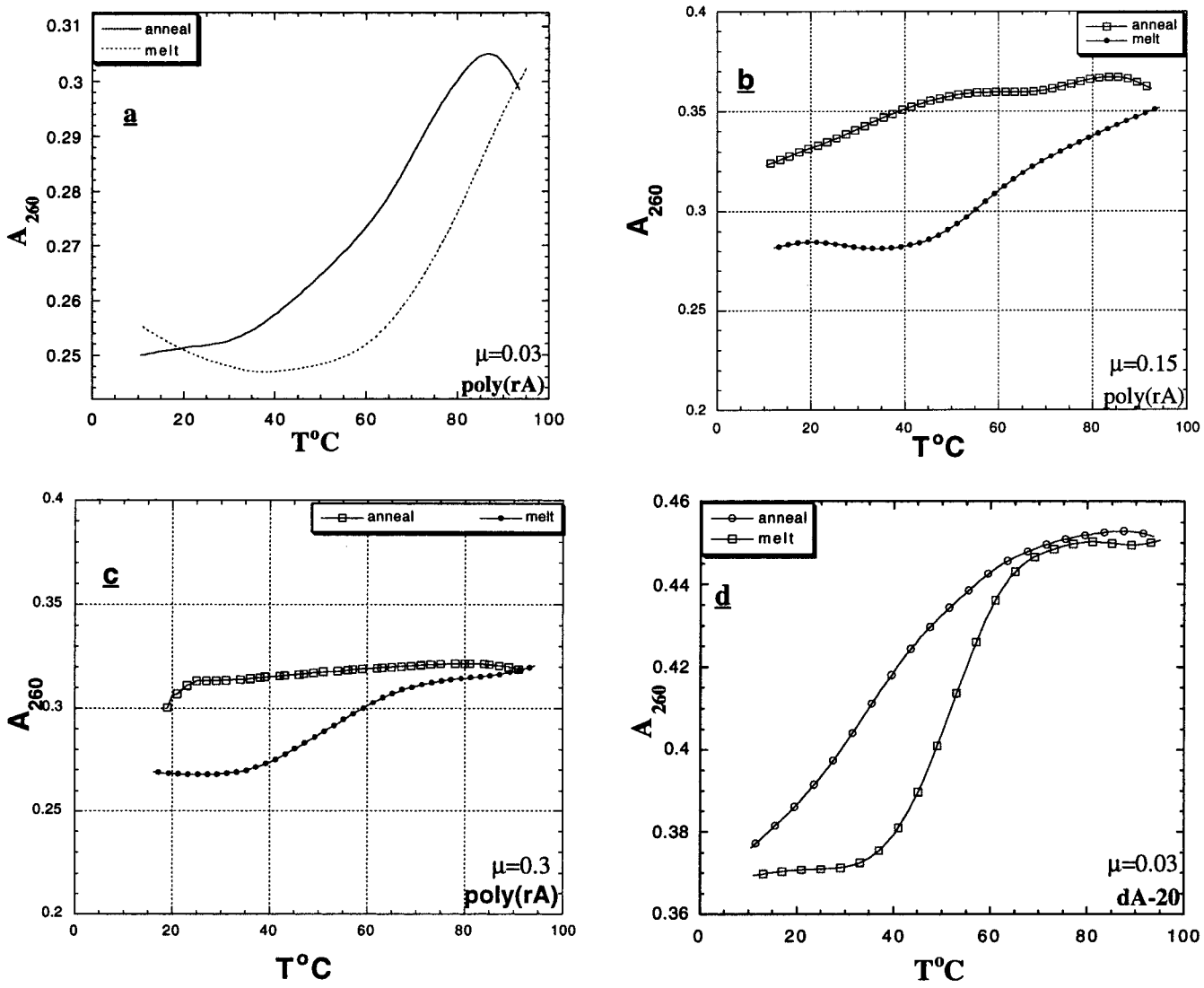

Figure 4. (a−c) Hysteresis curve of **11d** and poly(rA) in 8.5 mM K_2HPO_4 and 8.5 mM Na_2HPO_4KCl (pH 6.85) at different ionic strengths (μ = 0.06−0.3). (d) Hysteresis curve of **11d** and dA-20 in 8.5 mM K_2HPO_4 and 8.5 mM Na_2HPO_4KCl (pH 6.85) at an ionic strength of 0.03 (KCl). Data were recorded every 0.4°. The samples were heated from 25 to 95 °C at 5 deg/min, the annealing (95−5 °C) and the melting (5−95 °C) were conducted at 0.13 deg/min, and the reaction solutions were equilibrated for 15 min at the highest and lowest temperatures.

for DNmt bound to RNA and DNA with results of others for DNA bound to modified nucleotides (Figure 7). The plots of T_m/base pair of DNG·RNA duplex and DNG·RNA triplex[15,41] as a function of μ are also presented for comparison. While DNmt binds to poly(rA) and poly(dA) over a wide range of ionic strengths, the binding is less strong than shown by DNG. The effect of increasing μ on the destabilization of DNmt·DNA and DNmt·RNA complexes is much more pronounced compared to DNA·RNA duplexes which become more stable with an increase in μ.

Conclusion

Replacement of the phosphodiester linkages of DNA with methylthiourea linkages provides the polycation deoxyribonucleic methylthiourea (DNmt). The thermal denaturation analysis of **11d** {5′-NH_3^+-T_{mt}-$(T_{mt})_4$-OH} bound to poly(rA) and poly(dA) exhibits pronounced hysteresis. The DNG polycation-d$(Tg)_4$-T-azido[15,41] has been shown to bind to poly(dA) and poly(rA) with unprecedented affinity and with base-pair specificity to provide both double- and triple-stranded helices. Positively charged DNmt, similarly has a significantly greater affinity for poly(dA) and poly(rA) than does the DNA equivalent. The effect of ionic strength on melting is more pronounced with DNmt interacting with poly(A) and has an opposite effect as compared to DNA complexes with DNA or RNA. This is due, of course, to electrostatic interactions being attenuated by increasing salt concentrations. Earlier works in this laboratory show that the T_m of the double helix of pentameric thymidyl DNA with poly(dA) at μ = 0.12 is ca. 13 °C,[41] whereas the DNmt duplex with poly(dA) is estimated to be greater than 80 °C. At an ionic strength of 0.03, on the other hand, the five bases of DNmt are estimated to dissociate from a double helix with poly(rA) at >80 °C. A comparison with other positively charged oligonucleotides, ethylmorpholino phosphoramidate (T_m/bp = 2−3) and aminomethyl phosphonate (T_m/bp = 2−3),[31] containing positively charged ammonium groups connected via an alkyl linkage (Scheme 1, S6) to the central phosphorus atom of the backbone) and DNG (guanido-linked backbone, T_m/bp = 15−25) shows that the melting temperatures for DNmt complexes are much higher than the morpholino- or aminomethyl-linked oligos. This implies that, like DNG, DNmt maintains its positive charge in proper alignment to maximize its interaction with the backbone of the negatively charged phosphates of the opposite strand. On comparison with DNG,

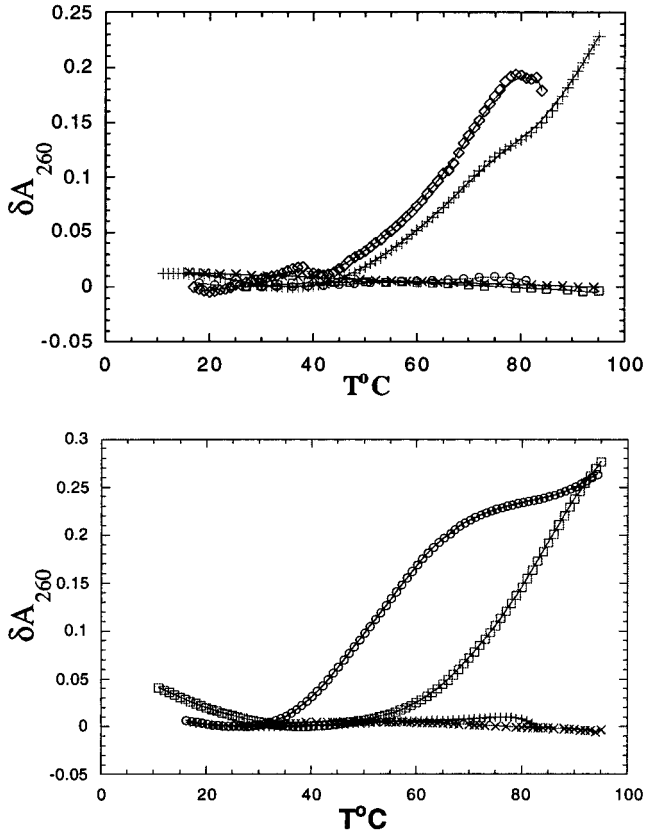

Figure 5. (a) Plots of A_{260} vs T (°C) for (**11d**) annealed to poly(dA) (+) at $\mu = 0.03$ (KCl), poly(dA) (◇) at $\mu = 0.3$ (KCl), poly(dG) (□), poly(dC) (×), and poly(dT) (○) in 8.5 mM K_2HPO_4 and 8.5 mM Na_2HPO_4 (pH 6.85) and an ionic strength of 0.15 (KCl). The concentration of each of the oligonucleotides was 2.17×10^{-5} M in bases. The ratio of **11d** to polynucleotides was 2:1. (b) Plots of A_{260} vs T (°C) for (**11d**) annealed to poly(rA) (□) at $\mu = 0.05$ (KCl), poly (rA) (○) at $\mu = 0.12$ (KCl), poly(rC) (+), poly(rG) (×) in 8.5 mM K_2HPO_4 and 8.5 mM Na_2HPO_4 (pH 6.85) and an ionic strength of 0.15 (KCl). The concentration of each of the oligonucleotides was 2.17×10^{-5} M in bases. The ratio of **11d** to polynucleotides was 2:1.

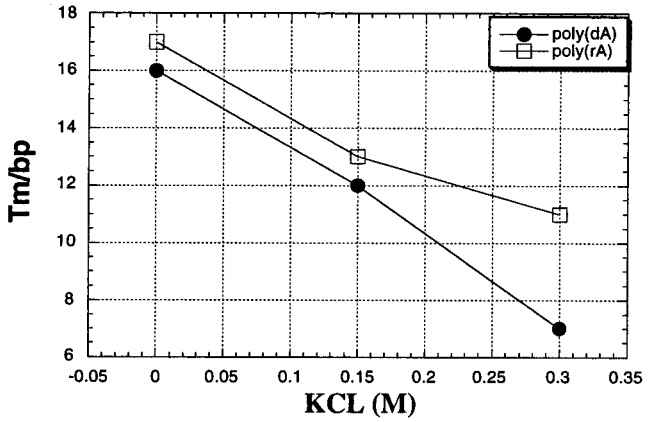

Figure 6. Plot of T_m of **11d**$_2$:poly(rA)/poly(dA) triplexes as a function of ionic strength in 8.5 mM K_2HPO_4 and 8.5 mM Na_2HPO_4 (pH 6.85). The concentration of each of the oligonucleotides was 2.17×10^{-5} M in bases. The ratio of **11d** to polynucleotides was 2:1.

the DNmt complexes are found to melt at a lower temperature (Figure 7). The fact that DNmts bind less tightly, than the guanido compounds (DNGs), provides a measure of the strength of control of binding with our cationic oligonucleotides. Specifically, at low μ, a 5-mer of DNG does not even come off poly(dA) in boiling water. Such strong electrostatic interactions

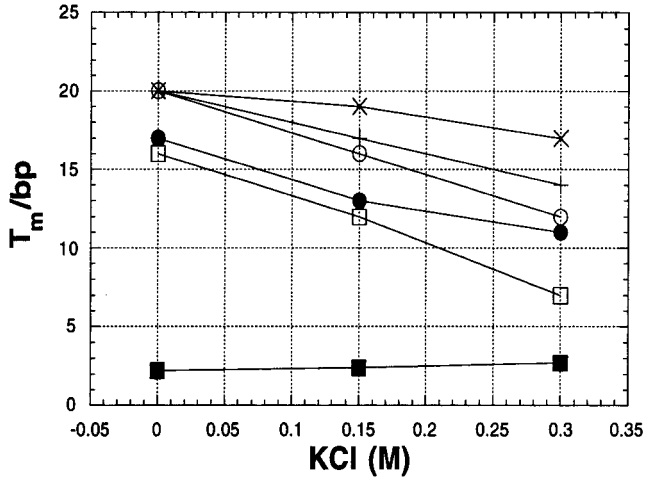

Figure 7. Plot of T_m per base pair vs μ in 8.5 mM K_2HPO_4 and 8.5 mM Na_2HPO_4 (pH 6.85). The plots are DNA. RNA duplex (■), DNG·RNA duplex (×), DNG·DNA (+), DNmt·RNA (●), and DNmt·DNA [first (○) and second transitions (□)]. The concentration of each of the oligonucleotides was 2.17×10^{-5} M in bases. The ratio of **11d** to polynucleotides was 2:1. Ionic strengths were held constant by adding potassium chloride. The data points at 100 °C for melting of DNG and DNmt complexes are approximations. The melting points for DNG·RNA complexes would be much higher than that for DNmt·RNA complexes.

would conceivably cause a loss of fidelity in binding for longer DNG sequences. The presence of an alkylated positively charged thiourea allows us to investigate the balance between charge, hydrophobicity, and fidelity. Conceivably, derivatives of DNmt wherein the methyl group has been replaced with other moieties to investigate the cell permeability and diffusion properties of these compounds should not alter the enhancement in binding as long as the positive charge rests on the backbone as opposed to the linkers that are tethered to it.[53]

From these results, the following conclusions can be drawn about DNmt: (a) Thymidyl DNmt has much stronger affinity for DNA and RNA, due to electrostatic attractions, than DNA for RNA or vice versa. (b) Thymidyl DNmt is specific for its complementary tracts of adenine bases and does not interact with guanylic, cytidylic, or uridylic tracts. (c) The thermal stability of DNmt·RNA and DNmt·DNA structures is attenuated by increasing salt concentrations. (d) DNmt forms triple helical structures from 15 to 60 °C that are very stable under physiological ionic strength conditions. (e) DNmt binding to poly(rA) is stronger than that to poly(dA). (f) DNmt oligos can be synthesized with relative ease, have an achiral backbone linkage, and would be stable to enzymatic hydrolysis due to the lack of a phosphodiester linkage.

Acknowledgment. This work was supported by a grant from the National Institutes of Health.

Supporting Information Available: Job plot of **11d** and poly(rA) at 60 °C, HPLC chromatograms of methylthiourea **6** and **11c,d**, FAB and ESI mass spectrum of **11d**, ^{1}H NMR and COSY spectrum of dimer **6**, and text describing experimental procedures and characterization of compounds **9b,c** and **11b,c** (9 pages, print/PDF). See any current masthead page for ordering information and Web access instructions.

JA9829416

(53) The comparisons in melting point differences presented are however of a qualitative nature and should not be overinterpreted (as pointed out by the reviewer) to conclude trends in the thermodynamic stability of these different backbone-modified oligos.